Indoor Air 1994, 4: 154–168
Printed in Denmark · all rights reserved

Indoor Air
ISSN 0905-6947

Numerical Method for a Full Assessment of Indoor Thermal Comfort

Guohui Gan[1]

Abstract

Heat, mass and momentum transfer takes place simultaneously in ventilated rooms. For accurate predictions of the indoor environment, all the environmental parameters that influence these transport phenomena should be taken into consideration. This paper introduces a method for a full assessment of indoor thermal comfort using computational fluid dynamics in conjunction with comfort models. A computer program has been developed which can be used for predicting thermal comfort indices such as thermal sensation and draught risk. The sensitivity of predicted comfort indices to environmental parameters is analysed for a mechanically ventilated office. It was found that when the mean radiant temperature was considered uniform in the office, the error in the predicted percentage of dissatisfied (PPD) could be as high as 7.5%. The prediction became worse when the mean radiant temperature was taken to be the same as air temperature point by point in the space. Moreover, disregarding the variation of vapour pressure in the space resulted in an error in PPD of abour 4% near the source of moisture generation.
The importance of evaluating both thermal sensation and draught risk is also examined. It is concluded that in spaces with little air movement only the thermal sensation is needed for evaluation of indoor thermal comfort whereas in spaces with air movement induced by mechanical vantilation or air-conditioning systems both thermal sensation and draught risk should be evaluated.

KEY WORDS:
Thermal comfort, Draught, Computational fluid dynamics (CFD), Air velocity, Mean radiant temperature, Vapour pressure

Manuscript received: 31 August 1993
Accepted for publication: 21 March 1994

[1] Department of Construction Management and Engineering, University of Reading, Whiteknights, Reading RG6 2AW, United Kingdom (Fax: 44 0734 313856)

Present address:
Institute of Building Technonogy
School of Architecture
University of Nottingham NG7 2RD, UK

Introduction

In the last few decades significant advances have been made in the understanding of indoor thermal comfort mechanisms. A number of indices have been introduced to describe the thermal environmental conditions and used in standards and guidelines for design and evaluation of thermal comfort. These include the operative temperature (ASHRAE, 1981), effective temperature (ASHRAE, 1985) and dry resultant temperature (CIBSE, 1986). Fanger (1982) has derived a set of the most comprehensive thermal sensation indices (PMV and PPD) to date, based on the heat transfer mechanism and extensive laboratory testing. His results have been adopted as an international standard (ISO, 1984) for the specification of indoor thermal comfort conditions. Recognising that draught is one of the most common causes of complaint in ventilated or air-conditioned buildings, Fanger (1993) recently emphasised that draught risk should be considered to be one of the indices for assessing thermal comfort and that the existing thermal comfort standards need to be updated to include the draught model (Fanger, et al., 1988). Thermal comfort in this paper refers to an acceptable thermal sensation level without risk of draught and without thermal discomfort due to either asymmetric radiation or vertical temperature gradient.

Indoor thermal comfort is to a large extent influenced by airflow behaviour in the space. Traditionally, the indoor airflow behaviour is assessed through laboratory or site measurements of air velocity and temperature distribution. Recently computational fluid dynamics (CFD) has been applied for predicting airflow in buildings and evaluating the indoor environment – thermal comfort and air quality. Examples of such applications can be found in the proceedings of two recent international conferences on room air movement (Anon. 1992a, b).

Numerical assessment of thermal comfort can be

performed through different approaches, depending on the comfort indices employed. Draught risk, for example, has been used as an index to evaluate thermal comfort in buildings (Chen, 1990). The author and his colleagues (Gan, et al., 1991; 1993b) have developed a CFD program for evaluating the indoor environment in ventilated rooms. The program produces thermal sensation indices, the Predicted Mean Vote (PMV) and the Predicted Percentage of Dissatisfied (PPD). Further development of the program has been made to enable both thermal sensation and draught risk indices to be predicted. In this paper, the principles of the program are described. The effect of the environmental parameters such as mean radiant temperature and water vapour pressure on the predicted thermal comfort indices is then assessed. Finally, the necessity for evaluating both the thermal sensation and draught risk in buildings is discussed.

Theory

The theoretical background and the main equations which are solved in order to predict the thermal comfort indices are described in this section. The airflow model, which is based on computational fluid dynamics (CFD), is described first, followed by the models for thermal sensation and draught risk.

Airflow Model

The fundamental airflow model consists of the continuity equation, Navier-Stokes (momentum) equation, enthalpy equation and concentration equation together with the k-ε turbulence model equations. For an incompressible steady-state flow, the time-averaged equations are as follows:

Continuity

$$\frac{\partial}{\partial x_i}(\varrho U_i)=0 \tag{1}$$

Momentum

$$\begin{aligned}\frac{\partial}{\partial x_i}(\varrho U_i U_j) &= \frac{\partial}{\partial x_i}\left((\mu+\mu_t)\left(\frac{\partial U_i}{\partial x_j}+\frac{\partial U_j}{\partial x_i}\right)\right)\\ &\quad -\frac{\partial}{\partial x_j}\left(p+\frac{2}{3}\varrho k\delta_{ij}\right)+g_i(\varrho_r-\varrho)\end{aligned} \tag{2}$$

Enthalpy

$$\frac{\partial}{\partial x_1}(\varrho U_i H)=\frac{\partial}{\partial x_i}\left(\left(\frac{\mu}{\sigma}+\frac{\mu_t}{\sigma_t}\right)\frac{\partial H}{\partial x_i}\right)+q \tag{3}$$

Concentration

$$\frac{\partial}{\partial x_i}(\varrho U_i C)=\frac{\partial}{\partial x_i}\left(\left(\frac{\mu}{\sigma_s}+\frac{\mu_t}{\sigma_c}\right)\frac{\partial C}{\partial x_i}\right)+C_s\varrho \tag{4}$$

In applying the concentration equation, it is assumed that either the size of concentration particles is so small or the density of concentration is so close to the density of dry air that there is no difference in flow velocity between air and concentration.

Air temperature. For a mixture of dry air and water vapour, the temperature of air is calculated from the enthalpy of the air mixture and the concentration of water vapour using (ASHRAE, 1985)

$$T=\frac{H-2501000C}{1000+1805C} \tag{5}$$

The units for the independent variables (H and C) in the above equation are originally based on mass of dry air but are expressed here on the basis of mass of air mixture. In doing so it is assumed that the specific heat of dry air is approximately equal to 1000 J/kg K for low concentrations.

Equation of state for an ideal gas mixture

$$\begin{aligned}\varrho &= \frac{p_a M_a + p_v M_v}{R\,(T+273.15)}\\ &= \frac{p_{at} M_a}{R\,(T+273.15)}\frac{1}{1+\left(\frac{M_a}{M_v}-1\right)C}\end{aligned} \tag{6}$$

This equation can be used for deriving the term representing buoyancy forces in the momentum equation, $g_i\,(\varrho_r-\varrho)$, in terms of temperature and concentration as follows:

Although the density of moist air is a function of not only air temperature and vapour concentration but also atmospheric pressure, the variation of atmospheric pressure is negligible in a microclimate such as the room environment. Therefore, by making a double Taylor series expansion of ϱ in terms of T and C, Equation 6 becomes

$$\varrho = \varrho_r - \varrho\,[\beta\,(T - T_r) + \beta_c\,(C - C_r)]$$

Hence,

$$g_i\,(\varrho_r - \varrho) = g_i\varrho\,[\beta\,(T - T_r) + \beta_c\,(C - C_r)] \tag{7}$$

where

$$\beta = -\frac{1}{\varrho}\left(\frac{\partial \varrho}{\partial T}\right)_{C,Pat} = \frac{1}{T_r + 273.15}$$

$$\beta_c = -\frac{1}{\varrho}\left(\frac{\partial \varrho}{\partial C}\right)_{T,Pat} = \frac{\dfrac{M_a}{M_v} - 1}{1 + \left(\dfrac{M_a}{M_v} - 1\right) C_r}$$

and subscript r is associated with the value of a variable at a reference point.

Turbulent viscosity

$$\mu_t = C_\mu \varrho \frac{k^2}{\varepsilon} \tag{8}$$

Turbulent kinetic energy

$$\frac{\partial}{\partial x_i}(\varrho U_i k) = \frac{\partial}{\partial x_i}\left(\left(\mu + \frac{\mu_t}{\sigma_k}\right)\frac{\partial k}{\partial x_i}\right) + \mu_t \frac{\partial U_i}{\partial x_j}\left(\frac{\partial U_i}{\partial x_j} + \frac{\partial U_j}{\partial x_i}\right) - C_d \varrho \varepsilon + G \tag{9}$$

Dissipation rate of turbulent kinetic energy

$$\frac{\partial}{\partial x_i}(\varrho U_i \varepsilon) = \frac{\partial}{\partial x_i}\left(\left(\mu + \frac{\mu_t}{\sigma_\varepsilon}\right)\frac{\partial \varepsilon}{\partial x_i}\right) + C_1 \mu_t \frac{\partial U_i}{\partial x_j}\left(\frac{\partial U_i}{\partial x_j} + \frac{\partial U_j}{\partial x_i}\right)\frac{\varepsilon}{k} - C_2 \varrho \frac{\varepsilon^2}{k} + C_3 G \frac{\varepsilon}{k} \tag{10}$$

where G is the buoyancy generation/destruction term which represents the combined effects of thermal and concentration diffusions and is given by

$$G = g_i\left(\beta \frac{\mu_t}{\sigma_t}\frac{\partial T}{\partial x_i} + \beta_c \frac{\mu_t}{\sigma_c}\frac{\partial C}{\partial x_i}\right)$$

This and other terms of Equations 9 and 10 are derived directly from Equation 2 with the aid of Equation 7. In the derivation, use is made of the Boussinesq approximation.

In the above equations, C is the mean concentration of water vapour in air (kg/kg); C_s is the concentration generation rate per unit volume ($m^3/s\ m^3$); g_i is the gravitational acceleration in x_i direction (m/s^2); H is the specific enthalpy for an air mixture (J/kg); k is the turbulent kinetic energy (m^2/s^2); M_a and M_v are the molecular weights of dry air and water vapour respectively (kg/mol); p is the static pressure of air (Pa); p_a and p_v are the partial pressures of dry air and water vapour, respectively (Pa); P_{at} ($=p_a+p_v$) is the atmospheric pressure (Pa); q is the volumetric rate of heat production (W/m^3); R is the universal gas constant (8.314 J/mol K); T is the mean air temperature (°C); U_i is the mean velocity component in x_i direction (m/s); β is the volumetric coefficient of thermal expansion (1/K); β_c is the volumetric coefficient of expansion with concentration; δ_{ij} is the Kronecker delta ($\delta_{ij}=1$ if i=j and $\delta_{ij}=0$ if $i \neq j$); ε is the dissipation rate of turbulent kinetic energy (m^2/s^3); μ and μ_t are the laminar and turbulent viscosities, respectively (kg/m s), ϱ is the air density (kg/m^3); σ and σ_s are the laminar Prandt1 number and Schmidt number, respectively; σ_t and σ_c are the turbulent Prandt1 number and Schmidt number, respectively. The following values are adopted for the empirical turbulence constants and turbulent Prandt1/Schmidt numbers:

$C_\mu=0.09$; $C_d=1.0$; $C_1=1.44$; $C_2=1.92$; $C_3=1.0$;
$\sigma_t=0.9$; $\sigma_c=1.0$; $\sigma_k=1.0$; $\sigma_\varepsilon=1.22$.

Boundary Conditions

To obtain a solution of the above equations, the room boundary conditions must be specified. These are either known quantities or empirical and semi-empirical expressions. The room boundary conditions for momentum, heat and moisture transfer are as follows.

Supply opening. The velocity, enthalpy (or temperature and humidity) of supply air are given as known values. The turbulent kinetic energy k_0 and its dissipation rate ε_0 of air at the supply outlet are calculated from

$$k_0 = 0.05\,V_0^2 \text{ and } \varepsilon_0 = \frac{C_\mu k_0^{1.5}}{0.07\,L}$$

where V_0 is the air velocity at the supply opening (m/s) and L is the length scale taken to be the slot width of the supply opening (m).

The pressure at the supply outlet is set to zero as a reference value for the purpose of computation.

Exit opening. The air velocity, enthalpy and humidity at the exit are obtained from the continuity equation, thermal energy and moisture concentration balance equations respectively. The pressure at the exit need not be specified since it is used only for the intermediate computation of the velocity. Other quantities such as the gradients of the turbulent kinetic energy and its dissipation rate are taken as zero.

Solid surface boundary. The wall surface temperature is normally specified. However, when there exists a heat gain/loss through a surface by conduction, convection or radiation it is computed from the heat transfer rate. Figure 1 illustrates the heat transfer through an external wall exposed to a cold ambient. The method involved in such a computation is described later in this section. In either case, at the boundary of a wall surface the following wall-function equations due to Launder and Spalding (1974) are used for the calculation of the velocity parallel to the boundary and convective component of heat flux through the wall:

for $y^+ \leq 11.63$: $u^+ = y^+$ and $T^+ = \sigma y^+$

for $y^+ > 11.63$: $u^+ = \frac{1}{\kappa} \ln (Ey^+)$ and

$$T^+ = \sigma_t \left[u^+ + f\left(\frac{\sigma}{\sigma_t}\right) \right]$$

where

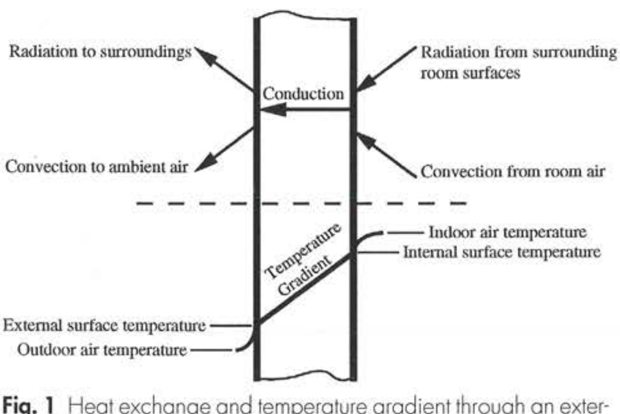

Fig. 1 Heat exchange and temperature gradient through an external wall in winter

E = logarithmic law constant (= 9.793)
κ = Karman's constant (= 0.4187)
y^+ = local Reynolds number ($y^+ = u_\tau \varrho y/\mu$)
u_τ = friction velocity ($u_\tau = \sqrt{(\tau_w/\varrho)}$)
τ_w = wall shear stress (Pa)
y = distance of a boundary grid point from a wall (m)
u^+ = dimensionless velocity ($u^+ = U_y/u_\tau$)
U_y = velocity parallel to a boundary (m/s)
T^+ = dimensionless heat flux temperature ($T^+ = \varrho u_\tau C_p (T_w - T)/q_w$)
C_p = specific heat of air at constant pressure (J/kg K)
q_w = convective component of heat flux through a wall (W/m^2)
T_w = wall surface temperature (°C)

$f(\sigma/\sigma_t)$ is given by Jayatillaka (1969):

$$f\left(\frac{\sigma}{\sigma_t}\right) = 9.24 \left[\left(\frac{\sigma}{\sigma_t}\right)^{0.75} - 1 \right] \times \left[1 + 0.28 \exp\left(-0.007 \frac{\sigma}{\sigma_t}\right) \right]$$

The solid walls are assumed to be impervious to moisture transfer, i.e. zero gradient of water vapour concentration normal to the boundary. However, when condensation on a surface takes place, a wall function similar to that for convective heat transfer is used for moisture transfer based on the heat and mass analogy. This is implemented simply by replacing T^+ with C^+ and Prandtl numbers (σ and σ_t) with Schmidt numbers (σ_s and σ_c). Here C^+ is the dimensionless mass flux and is given by

$$C^+ = \frac{u_\tau (C_w - C)}{N}$$

where C_w is the concentration of water vapour at the wall surface in contact with air (kg/kg) and N is the rate of mass transfer (m/s).

In the calculation of condensation, C_w is taken as the saturation water vapour concentration at the temperature of the wall surface and the water vapour concentration at the boundary C is obtained from the wall function C^+. The enthalpy of moist air at the boundary is then obtained from the enthalpy for dry air and that for water vapour. The latent heat released in condensation of the moisture is taken into consideration in calculating the room surface temperature.

The turbulant kinetic energy and its dissipation rate at the boundary are calculated from

$$k = \frac{U_\tau^2}{\sqrt{C_\mu}} \quad \text{and} \quad \varepsilon = \frac{U_\tau^3}{\kappa y}$$

The treatment of the wall boundary is also applied to the surface of obstacles such as occupants and furniture in the room.

Table 1 summarises the boundary conditions used for simulation.

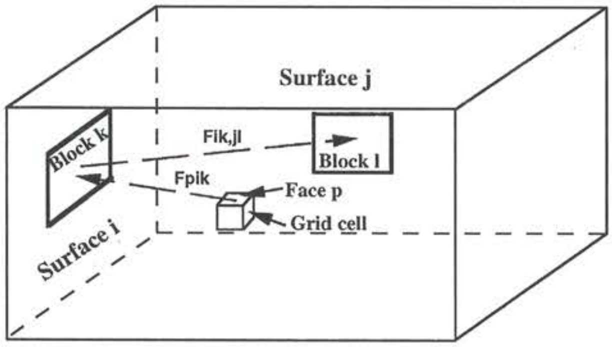

Fig. 2 Schematic representation of the evaluation of shape factors

Solution Method

The airflow model equations are solved for the three-dimensional cartesian system using the SIMPLE algorithm (Patankar, 1980). In this method, the partial differential equations are directly discretised by means of a finite volume technique on a staggered grid. A QUICK scheme (Leonard, 1979) is used for the solution of momentum equations and a hybrid (upwind/central) differencing scheme for other transport equations. To enhance the stability of the solution, under-relaxation factors are applied to all the equations.

Validation of the airflow model has been carried out for the predicted velocity, temperature and concentration distributions in ventilated rooms (Awbi and Gan, 1991; Gan, et al., 1993a).

Thermal Sensation

Thermal sensation is evaluated in terms of the predicted mean vote and the predicted percentage of dissatisfied proposed by Fanger (1982). These indices take account of the combined effect of environmental conditions such as air velocity, air temperature, mean radiant temperature and partial water vapour pressure of air and the occupants' conditions such as clothing and activity levels. In this study the air velocity, temperature and water vapour pressure (concentration) distributions in a room are calculated from the flow equations. The distribution of mean radiant temperature is attained with the help of a radiation heat exchange model.

Table 1 Boundary conditions for simulation

Variable	Supply opening	Exit opening	Solid boundary
U_i	Specified V_0	Continuity	Calculated from u^+
H or T	Specified	Heat balance	Specified or calculated from T^+
C	Specified	Contentration balance	$\partial C/\wp n=0$ or calculated from C^+
k	$k_0=0.05\ V_0^2$	$\partial k/\partial n=0$	$k=u_\tau^2/\sqrt{C_\mu}$
ε	$\varepsilon_0=\dfrac{C_\mu k_0^{1.5}}{0.07\ L}$	$\partial\varepsilon/\partial n=0$	$\varepsilon=u_\tau^3/\kappa y$

where n is the normal distance from the wall

Room Surface Radiosity

The radiosity is the rate at which total radiant energy leaves a surface per unit area. The calculation of the mean radiant temperature is based on the radiosity of room surfaces. Each surface of a room can be divided into a number of small blocks depending on the variation of the temperature or heat flux. The determination of the radiant heat exchange between any two blocks is facilitated through the geometric shape factor. Figure 2 shows the configuration of shape factors between two surface blocks ($F_{ik,jl}$) and between a face of a grid cell and a surface block (F_{pik}). The radiosity J_{ik} (W/m^2) of block k of surface i at temperature T_{ik} is obtained from

$$J_{ik} = \varepsilon_{ik}\varsigma T_{ik}^4+(1-\varepsilon_{ik})\sum_{j=1}^{n}\sum_{l=1}^{m} F_{ik,jl}J_{jl} \tag{11}$$

where ε_{ik} is the emissivity of block k of surface i (namely surface block ik); ς is the Stefan-Boltzmann constant (5.67×10^{-8} W/m^{2}K^4); $F_{ik,jl}$ is the radiation shape factor for block k of surface i with respect to block 1 of surface j; m is the number of blocks of a room surface and n is the number of room surfaces.

If a radiant heat flux q_{ik} (W/m^2) is present on surface block ik then the radiosity is calculated using the following equation:

$$J_{ik} = q_{ik}+\sum_{j=1}^{n}\sum_{l=1}^{m} F_{ik,jl}J_{jl} \tag{12}$$

Room Surface Temperature

When a heat source or sink is present in a room, the heat transfer to the room air takes place by convection and to the room surfaces by radiation as well as to the room fabric by conduction. It is then required to calculate the temperatures of inner room surfaces and use these as boundary values in the CFD prediction. If the radiation heat transfer is negligible, the temperature for each surface can be calculated from the heat transfer rate. However, if the radiant heat source or sink in a room surface plays an important role, the temperatures of room surfaces must be obtained using a radiation heat exchange model.

For surface block ik with a radiant heat flux, the temperature T_{ik} is given by

$$T_{ik} = \left[\frac{1}{\varsigma}\left(J_{ik} + \frac{1-\varepsilon_{ik}}{\varepsilon_{ik}} q_{ik}\right)\right]^{1/4} \tag{13}$$

If there is no radiant heat flux on surface block ik, Equation 13 is transformed to calculate the net radiant heat flow rate using

$$q_{ik} = \frac{\varepsilon^{ik}}{1-\varepsilon_{ik}} (\varsigma T_{ik}^4 - J_{ik}) \tag{14}$$

The surface temperature is then obtained from the heat balance equations for conduction, convection and radiation (see Figure 1) as well as the latent heat release in the case of condensation. Equations 11 through 14 are solved through iteration within each of the iterations for airflow equations.

Mean Radiant Temperature

In the calculation of mean radiant temperature at a grid point in the field, the grid cell is considered as a rectangular parallelepiped. The plane radiant temperature, T_{prt} (K), at each face of the cell is calculated from

$$T_{prt} = \left(\frac{1}{\varsigma} \sum_{i=1}^{n} \sum_{k=1}^{m} F_{pik} J_{ik}\right)^{1/4} \tag{15}$$

where F_{pik} is the radiation shape factor for radiation from face p of a grid cell to visible room surface block ik.

The mean radiant temperature, T_{mrt} (°C), for the grid cell is then taken as the average of the six plane radiant temperatures for each face of the rectangular parallelepiped weighted by the corresponding face areas.

Thermal Sensation Indices

The predicted mean vote, PMV, and predicted percentage of dissatisfied, PPD (%), are given by ISO (1984) as:

$$\begin{aligned} PMV = {} & [0.303e^{-0.036\,M} + 0.028]\ \{(M-W) \\ & - 3.05\times10^{-3}\times[5733-6.99\,(M-W)-p_v] \\ & - 0.42\,[(M-W)-58.15] \\ & - 1.7\times10^{-5}\,M\,(5867-p_v) \\ & - 0.0014\,M\,(34-T) \\ & - 3.96\times10^{-8}\,f_{cl}\,[(T_{cl}+273.15)^4 \\ & - (T_{mrt}+273.15)^4] \\ & - f_{cl}\,h_c\,(T_{cl}-T)\} \end{aligned} \tag{16}$$

and

$$\begin{aligned} PPD = {} & 100-95\exp(-0.03353\,PMV^4 \\ & - 0.2179\,PMV^2) \end{aligned} \tag{17}$$

where

$$\begin{aligned} T_{cl} &= 35.7-0.028\,(M-W)-I_{cl}\{3.96\times10^{-8}\,f_{cl} \\ &\quad \times [(T_{cl}+273.15)^4-(T_{mrt}+273.15)^4] \\ &\quad + f_{cl}\,h_c\,(T_{cl}-T)\} \\ h_c &= 2.38\,(T_{cl}-T)^{0.25} \\ &\quad \text{for } 2.38\,(T_{cl}-T)^{0.25} > 12.1\sqrt{V_r} \\ h_c &= 12.1\sqrt{V_r} \\ &\quad \text{for } 2.38\,(T_{cl}-T)^{0.25} < 12.1\sqrt{V_r} \\ f_{cl} &= 1.00+1.290\,I_{cl} \qquad \text{for } I_{cl} \le 0.078\ m^2K/W \\ f_{cl} &= 1.05+0.645\,I_{cl} \qquad \text{for } I_{cl} > 0.078\ m^2K/W \end{aligned}$$

f_{cl} is the ratio of man's surface area while clothed to the area while nude; h_c is the convective heat transfer coefficient (W/m^{2}K); I_{cl} is the thermal resistance of clothing (m^{2}K/W); M is the occupant's metabolic rate (W/m^2); p_v is the partial pressure of water vapour in air (Pa); T is the air temperature (°C); T_{cl} is the surface temperature of clothing (°C); T_{mrt} is the mean radiant temperature (°C); W is the external work accomplished (W/m^2) and V_r is the relative air velocity (m/s).

Although the PMV and PPD models are derived for predicting the thermal sensation for the body as a whole, based on a uniform thermal climate in the occupied zone of a room, these indices can be used to analyse the thermal variability in the room for given environmental variables (Fanger, 1982). Thus, even if the average values for PMV and PPD in the occupied zone are such that thermal sensation is acceptable, the value for PPD near the floor for example may be higher than 10% due to non-uniform distribution of environmental parameters and consequently there will be local discomfort from unsatisfactory thermal conditions. The environmental parameters then need to be adjusted in order to achieve a satisfactory thermal environment.

In addition to the calculation of thermal sensation, radiant temperature asymmetry for three orthogonal directions can be obtained from Equation 15. Local discomfort due to an asymmertric radiation field such as cold windows and hot radiators can then be evaluated.

Draught Risk

Fanger, et al. (1988) found that the sensation of draught is influenced not only by air temperature (T) and velocity (V) but also by the air turbulence level (Tu). They developed the following draught model which is used in this study to assess the draught risk, the percentage of dissatisfied due to draught (PD): for V>0.05 m/s,

$$PD = (3.143+0.3696\,V\,Tu)\,(34-T)\,(V-0.05)^{0.6223} \tag{18}$$

for $V \leq 0.05$ m/s, PD=0
and for PD>100%, set PD=100%.

The turbulence intensity, Tu (%), is defined as the standard deviation divided by the mean velocity of air in turbulent flow and can be calculated using

$$Tu = \frac{\sqrt{2k}}{V} \times 100 \tag{19}$$

Therefore, the distribution of PD in the space can be obtained from the solution of the airflow equations.

Application

The above theories are applied here for the prediction of thermal comfort in a low-cost energy-efficient office at the UK Building Research Establishment (BRE low-energy office). This is one of the standard offices recommended for use in modelling studies (Leighton and Pinney, 1990). In this section, results of one simulation are briefly discussed. The sensitivity of predicted thermal comfort levels to some parameters is then analysed.

Room Description

A schematic diagram of the office is shown in Figure 3. The office is 4.7 m long, 3.65 m wide and 2.5 m ceiling height. It consists of one external wall and five internal walls including the floor and ceiling. The external wall is precast concrete units clad with ceramic tiles, cavity approximately 0.3 m with 0.15 m insulation, timber framed inner skin with dry lining finish, giving a U-value (overall thermal transmission coefficient) of 0.22 W/m^{2}K. The U-value for internal walls is 1.70 W/m^{2}K. The external wall has a double-glazed window of width 2.95 m and height 1.3 m with a U-value of 2.9 W/m^{2}K. All the room surfaces are assumed to be grey and have an emissivity of 0.9. In winter the window is locked and the room is heated with a recirculating mechanical heating and ventilation system with heat recovered from the extract air transferred to the incoming air by means of a heat wheel. In summer the window is unlocked for natural ventilation. Simulation is carried out for the winter heating season. The outdoor design air temperature is −1 °C. Warm air is introduced vertically upwards from the heating system beneath the window. Part of the room air is returned through the recirculation grille at the bottom of the heater and the rest is extracted through an extract duct installed on the wall opposite to the curtain wall. The ventilation rate, including air infiltration, is four air changes per hour (i.e. 47.7 *l*/s), of which 22.5% is outdoor fresh air and the rest (77.5%) is recirculated air. To simplify the simulation, the air infiltrated into the room is considered as part of the supply air. The supply air is at a temperature of 23 °C and relative humidity of 40%.

The office is designed to minimise artificial lighting. This is achieved through maximum use of natural light from the large double-glazed window in conjunction with automatic lighting control. The observed rate of electric consumption for lighting over the room area is very small (on annual average, less than one Watt) (Crisp, et al., 1984). The heat provided by lighting is therefore ignored in the simulation.

The office is occupied by one person, seated by a desk and 1.2 m away from the window. The occupant and the desk are modelled as obstacles in the room. The simulated occupant generates metabolic heat of 70 W/(m^2 skin area) of which 30% is considered to be latent heat. The moisture production rate by the occupant is estimated from the amount of latent heat and is assumed to be a source at a grid point near the head level. The occupant wears clothes equivalent to a clothing level of 0.8 clo as a base value (1.0 clo=0.155 m^2K/W).

Computational details. The accuracy of a numerical solution is dependent on the grid size. A fine grid generally produces more accurate results than does a coarse grid. However, in many three-dimensional cases, because of the computing cost or the limitation of computer capacity, the fine grid mesh may not be easily achievable for the whole computational domain and instead a mixed grid of fine and coarse control volumes (cells) is often used. In general, relatively small cells should be provided in areas where large gradients of the solution variables occur such as in regions near the supply opening and solid boundary.

In this study, a grid of non-uniform intervals is employed, with the grid nodes concentrated near the walls and the heater which is close to the curtain wall anyway. The grid size is 38×36×30 (for room length, height and width directions) and it takes about 35 hours CPU time to solve the airflow equations for 800 iterations together with the comfort equations using Sun Sparc 1 workstation.

Simulation Results and Discussion

The simulation produces distributions of environmental parameters and thermal comfort indices in the space.

Environmental Parameters for Thermal Sensation
Figure 4 shows the predicted air movement and distributions of air temperature, mean radiant temperature and water vapour pressure on a vertical plane in the office. The location of the plane for plotting this figure and subsequent two figures is indicated in Figure 3. The upward air supply from the sill has overcome the potential downdraught and induced air circulation in the room. On the plane shown in Figure 4(a), air circulation occurs between the occupant and the wall with the extract duct due to deflection of the air stream by the occupant and thermal buoyancy from the body heat. The area between the heater and the occupant is very stagnant because of the blockage of air movement by the occupant. In sections where there is no obstruction to air movement, air circulation takes place around the room boundary in the same direction. The velocity

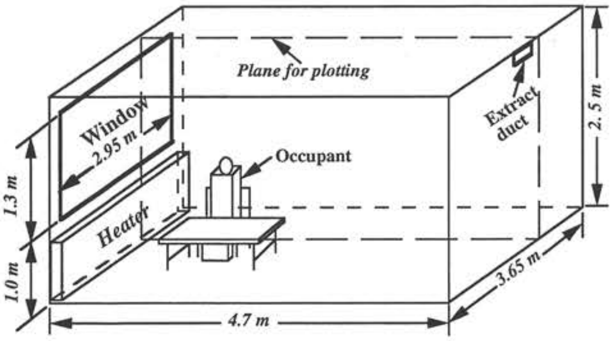

Fig. 3 Schemiatic diagram of the office with occupancy

in the room is overall very low, especially in areas away from the boundary and occupant. The average velocity in the occupied zone is only 0.04 m/s and the velocity for the whole space is 0.05 m/s, indicating stagnant air in the room. The *occupied zone* here is defined as the space from floor to a height of 1.8 m and 0.15 m away from side walls.

The air temperature is between 19.0 and 20.0 °C at foot level and is about 21.0 °C around the head with an average value of 20.4 °C for the occupied zone. The mean radiant temperature near the window is relatively low (<18.0 °C) due to heat loss through the window but is quite uniform about 1.0 m away from the curtain wall (between 18.5 and 19.0 °C). This relatively uniform radiant temperature distribution is the result of a small temperature difference between room surfaces (<10.0 K) owing to the use of double glazing. On the other hand, it is clear by comparison of Figure 4(c) with 4(b) that the radiant temperature distribution does not follow the pattern of air temperature. Hence taking mean radiant temperature as air temperature or a single value related to surface temperatures will lead to errors in prediction of thermal sensation indices as will be discussed below.

The vapour pressure of air in the space varies from 1120 Pa near the air supply opening to 1810 Pa at the source of moisture generation, with a mean value in the space of 1167 Pa. The apparent small variation of the vapour pressure seen from Figure 4(d) is due to the large quantity of air supplied in contrast with the low rate of moisture production. The relative humidity is between 40% at the supply opening and 70% near the moisture generation source, with a mean value in the occupied zone of about 49%. These extreme values for vapour pressure and relative humidity are confined only to very small areas around the air supply and

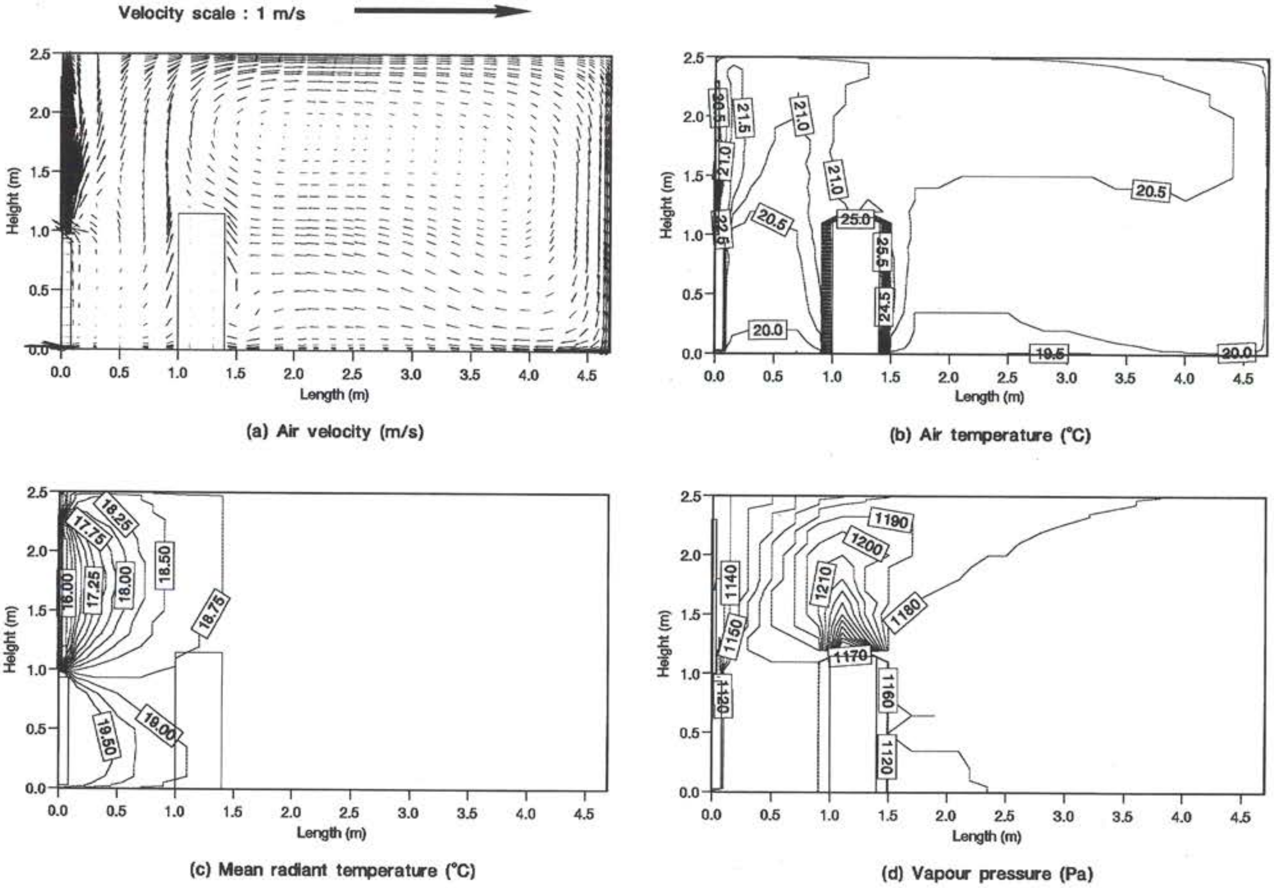

Fig. 4 Predicted environmental parameters for thermal comfort indices on a vertical plane in the office

the moisture generation source. Their variations are otherwise within 10% from the mean values for the whole space.

Although the cold window is expected to have the lowest room surface temperature, the numerical prediction shows that even here condensation will not occur, owing again to the double glazing.

Thermal Comfort Levels

Figure 5 shows the predicted thermal comfort levels on the same vertical plane as that for Figure 4. At the normal winter clothing level of 0.8 clo, discomfort can be expected especially at foot level and near the window (see Figure 5(b)) due to low air and radiant temperatures. The average PPD in the occupied zone is 16.4% and it is on the side of being cool as indicated by the negative PMV values in Figure 5(a). The thermal sensation level is thus unacceptable according to the ISO recommendation for PPD of 10% (ISO, 1984).

When the clothing level is increased from 0.8 clo to 1.0 clo (by adding a sweater for example), the thermal sensation level is improved as shown in Figure 6(a) compared with Figure 5(b). The calculated value for PPD in the occupied zone becomes 7.9%. Note that the values for the PPD contours in Figure 6 correspond to the percentage "cold dissatisfied", i.e. PMV<0. Therefore, for the existing heating system and heat supply rate, it is feasible to make use of clothing adjustment so as to achieve an acceptable thermal environment while keeping the heating costs low.

For this simulation, thermal discomfort due to asymmetric radiation or vertical temperature gradient is insignificant. The direction in which the discomfort due to asymmetric radiation may arise is obviously normal to the cold window. Figure 5(c) shows the radiant temperature asymmetry for this direction on the vertical plane. The value for a *radiant temperature asymmetry* in the direction discussed is defined as the difference between the plane radiant temperature for a grid cell facing the wall with the extract duct and that facing the curtain wall. The area near the window is the location where the

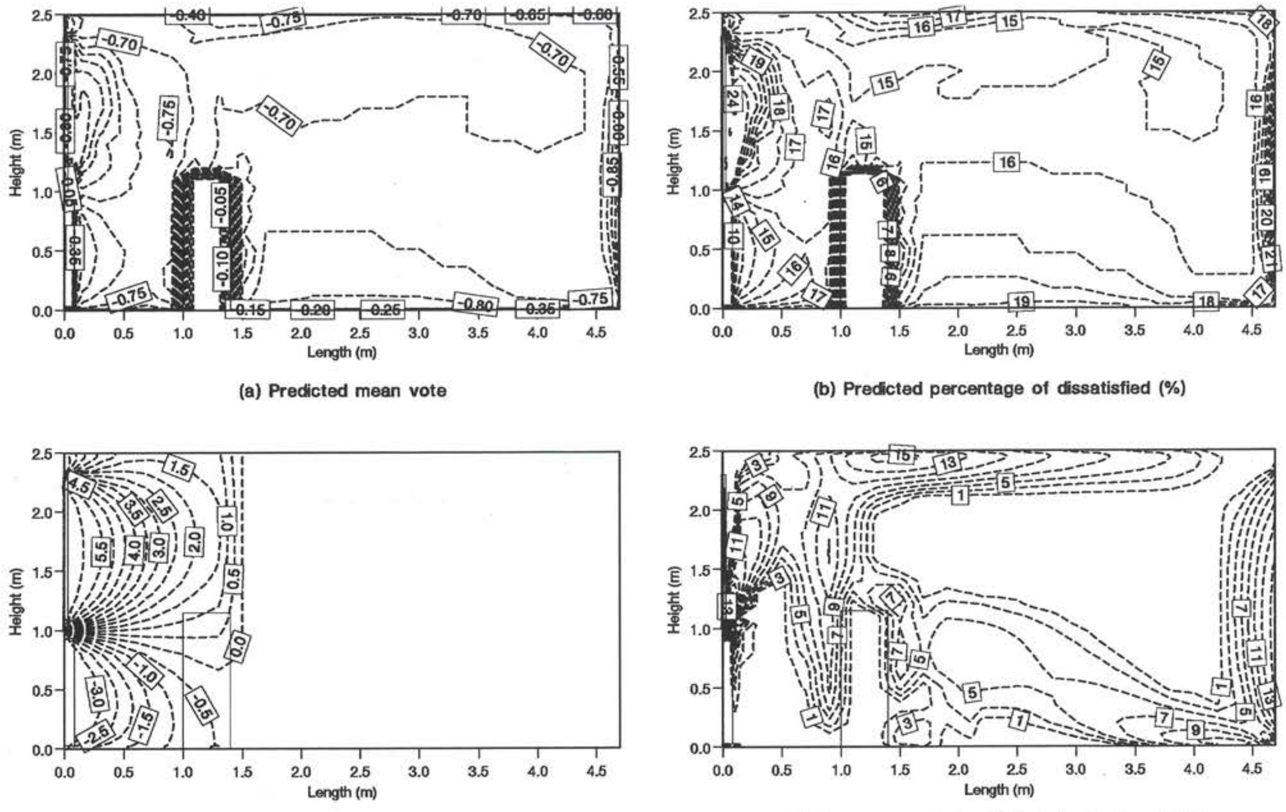

(a) Predicted mean vote

(b) Predicted percentage of dissatisfied (%)

(c) Radiant temperature asymmetry (K)

(d) Percentage of dissatisfied due to draught (%)

Fig. 5 Predicted thermal comfort indices on a vertical plane in the office

maximum radiant temperature asymmetry exists. The predicted value for this area (within the occupied zone) is 6.1 K. The radiant temperature asymmetry at the occupant's head region is only 1.0 K. The negative radiant temperature asymmetry near the heater indicates that plane radiant temperatures for grid cells in this area facing the heater are higher than those facing the opposite wall. The vertical temperature gradient between 1.1 m and 0.1 m above the floor is 0.5 K. Therefore, the asymmetric radiation and temperature gradient are both well within the comfort limits of 10.0 K and 3.0 K respectively (ISO, 1984).

The predicted draught risk above the head level is higher than that near the floor (Figure 5(d)). The calculated value for PD in the occupied zone is 5% approximately. This low level of PD is largely due to low air movement in the office. The air velocity in more than half of the occupied zone is below 0.05 m/s (average in the occupied zone is 0.04 m/s) and the corresponding PD value is zero according to Equation 18. Overall the draught risk is therefore small in the room. However, the PD value in the area right above the head exceeds 10%, which might cause some discomfort as the head is the most draught-sensitive region (Fanger, et al., 1988).

Effect of Environmental Parameters on Predicted Thermal Comfort Levels

Most CFD programs applied in room ventilation generate airflow patterns and temperature distribution in the space. The assessment of thermal sensation levels are usually based on the assumption of uniform distribution of other environmental parameters, namely, mean radiant temperature and water vapour pressure. In this section the sensitivity of the predicted comfort levels to the mean radiant temperature and water vapour pressure is analysed and possible errors arising from taking any of these two variables as a constant are estimated.

Mean Radiant Temperature

As mentioned earlier, the mean radiant temperature in the office is relatively uniform due to double glazing and forced air supply. Nevertheless, the accuracy in predicting comfort indices can still be affected by the way the mean radiant temperature is calculated. Because of the complexity of its calcu-

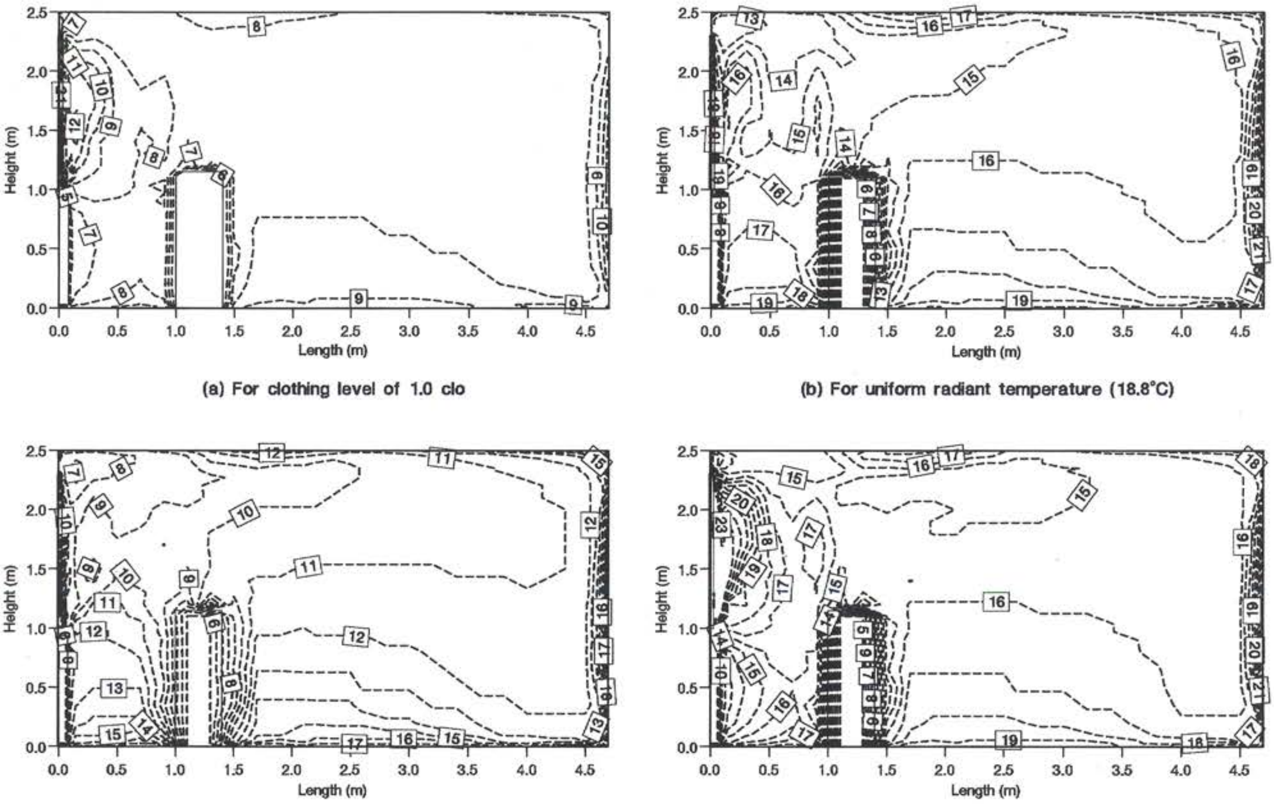

(a) For clothing level of 1.0 clo

(b) For uniform radiant temperature (18.8°C)

(c) For mean radiant temperature = air temperature

(d) For uniform vapour pressure (1167 Pa)

Fig. 6 Effect of personal and environmental parameters on the predicted thermal sensation levels on a vertical plane in the office

lation, the mean radiant temperature is often approximately taken as a single value related to surrounding surface temperatures and strictly speaking this is then used for the centre of the room only. There are at least two approaches to the approximation. One is to take the mean radiant temperature as a simple arithmetic mean of the surface temperatures weighted with the corresponding surface areas. The other is to calculate the mean radiant temperature from

$$T_{mrt} = \left(\frac{\Sigma(A_{ik}T_{ik}^4)}{\Sigma A_{ik}}\right)^{1/4} - 273.15 \qquad (20)$$

where A_{ik} is the area of surface block ik (m^2), T_{ik} is the absolute temperature of surface block ik in degree Kelvin whereas T_{mrt} is the mean radiant temperature in degree Celsius.

For the case studied, the difference in the mean radiant temperature using these two methods is negligible (<0.1 K) owing to the small difference in room surface temperatures (<10.0 K). However, if this single value is used to represent the distribution of radiant temperature for the whole space, significant errors in the predicted comfort levels will arise for areas where the approximate value deviates considerably from the calculated mean radiant temperature based on the exact heat transfer solution. This can be seen by comparison of the predicted comfort levels between Figure 5(b) and Figure 6(b). The latter is obtained using the approximated value of T_{mrt} (=18.8 °C) given by Equation 20 which is higher than the accurate value for the area near the cold window (<18.0 °C). As a result of the approximation, the PPD value, for example, on the edge of the occupied zone close to the window is reduced from 23.0% to 15.5% (corresponding to the PMV value from −0.92 to −0.71), 7.5% for PPD "warmer", though still on the cool side. Had the window been single-glazed, the error would have been much larger.

In certain circumstances such as parametric analysis of comfort equations, the mean radiant temperature may have to be approximately taken as air temperature due to unknown surroundings. The predicted thermal sensation indices will then be

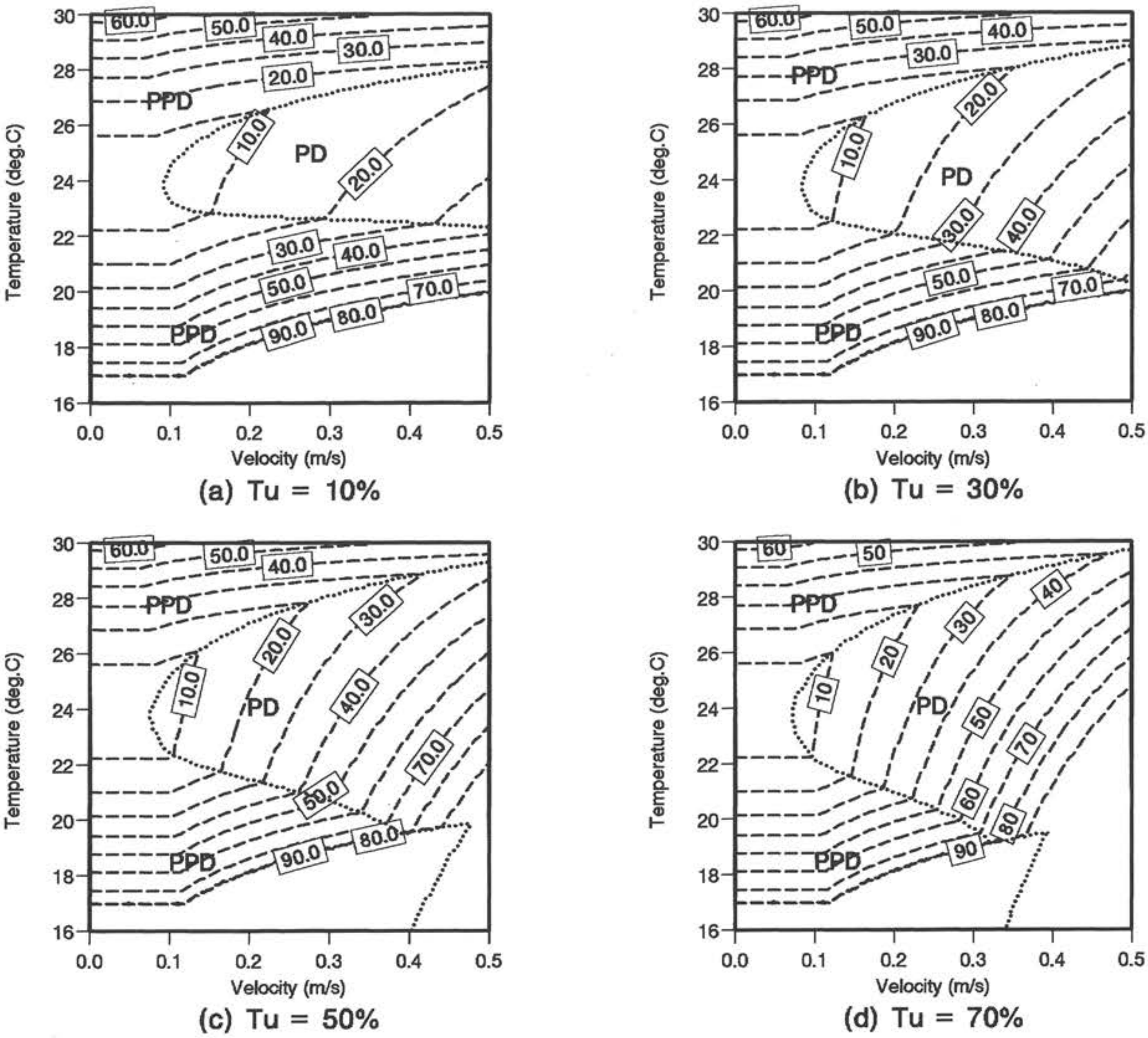

Fig. 7 Effect of air temperature and velocity on thermal comfort index Ψ=max [PPD, PD] for I_{cl}=0.6 clo

index PD and therefore Ψ=PPD. That is to say, if the requirement for PPD is the same as that for PD, draught will not be a cause of severe discomfort so long as the thermal sensation level is acceptable; hence using the thermal sensation index is sufficient for assessing thermal comfort provided that there is no other cause for thermal discomfort such as asymmetric radiation and excessive vertical temperature gradient. When the air velocity increases, however, draught is more likely to be the cause of thermal discomfort than is thermal sensation especially if the turbulence level is high and hence Ψ= PD.

With regard to thermal sensation, the figures are approximately symmetrical around air temperature (i.e. neutral temperature for air velocity <0.1 m/s) of about 24.0 °C and 22.5 °C for clothing levels of 0.6 clo and 1.0 clo respectively. Above the symmetrical line is the thermal discomfort due to warmth and below the line is the cold thermal discomfort. As air temperature moves away from the symmetrical line, the range of air velocity for Ψ= PPD, i.e. using thermal sensation as the only index for thermal comfort without considering the risk of draught, increases. For example, for the clothing level of 0.6 clo and at a turbulence intensity of 30%, the maximum air velocity for Ψ=PPD is about 0.08 m/s at the neutral temperature but increases to about 0.15 m/s at air temperature 2.0 °C higher or lower than the same neutral temperature.

Although the clothing level affects only thermal sensation, it alters the relative position of PPD and PD contours. As the clothing level increases, the effect of air velocity on thermal sensation decreases compromised. The compromise may not be acceptable for a known environment if air temperature distribution deviates substantially from that for mean radiant temperature. As an example, Figure 6(c) shows the predicted thermal sensation on the vertical plane in the office, obtained by taking the mean radiant temperature to be the corresponding air temperature for each grid point in the space. It is seen by comparing Figure 6(c) with Figure 5(b) that the distribution of predicted thermal comfort using air temperature as radiant temperature is totally different from that obtained using the radiation heat transfer model. This can be attributed to different distribution patterns for air temperature and mean radiant temperature. The air temperature increases gradually from floor to ceiling due to buoyancy whereas the mean radiant temperature near the cold window is lower than that for the rest of the space. Therefore, for accurate predictions, the mean radiant temperature should not be compromised as air temperature in surroundings with non-uniform surface temperatures, particularly in air-conditioned perimeter offices or rooms heated with a mechanical ventilation system.

Water Vapour Pressure

Figure 6(d) shows the predicted thermal sensation on the vertical plane using a constant vapour pressure (p_v=1167 Pa, predicted mean value for the whole space). It can be seen in comparison with Figure 5(b) for variable vapour pressure that overall the error in predicting thermal sensation levels is small (within 1.0% for PPD) by taking vapour pressure as a constant. The reason for this very small difference is that the variation of vapour pressure in the space, except the area around the moisture generation source, is small and above all that, for relative humidity of air between 30% and 70%, the influence of vapour pressure on the predicted thermal sensation indices is not as significant as other environmental parameters. At the source of moisture generation, however, the predicted values for PMV and PPD are −0.68 and 14.8% respectively for p_v=1167 Pa compared with −0.52 and 10.7% for p_v=1810 Pa (given by the solution of the airflow equations), a net increase in PPD of 4.1% using a constant vapour pressure (cooler than it should be). The area near the moisture generation source (close to the occupant!) is one of the most important areas for occupant comfort and hence the prediction of comfort levels should be as accurate as possible. Yet, it is also the area where the largest error occurs when the variation of vapour pressure with space is neglected.

Hence, it may be said that for accurate predictions of thermal sensation indices the variation of vapour pressure with space needs to be taken into account for a known indoor occupancy pattern. This is particularly important for places such as classrooms and auditoria where the occupancy density is high or places where there might be moisture production sources other than occupants and hence the variation of humidity with space could be large. However, for a space with no internal moisture generation source, comfort indices can be predicted using a constant but realistic vapour pressure without much loss of accuracy.

Comparison Between PPD and PD

The thermal sensation index PPD and draught risk index PD are both dependent on several parameters. Some parameters such as air temperature and velocity are common to both PPD and PD whereas others are relevant to only one of the indices. If the requirement for percentage of occupants' satisfaction with thermal sensation is the same as that for draught risk, a new index may be used to represent both PPD and PD. This new index is here defined as

$$\Psi = \max\,[\mathrm{PPD}, \mathrm{PD}] \tag{21}$$

That is, Ψ is equal to the higher value of PPD and PD. Using this index, the influence of the parameters on the variations of PPD and PD can easily be analysed. Figures 7 and 8 show the effect of air temperature and velocity on Ψ (the variations of PPD and PD) at four turbulence levels for two clothing levels of 0.6 clo and 1.0 clo. These Ψ contour plots are obtained for each combination of the independent variables under the following assumptions:

1) occupants at a sedentary activity level (1.2 met $\approx$ 70 W/m^2 skin area);
2) mean radiant temperature=air temperature;
3) relative humidity of air=50%.

The line in which PPD and PD intersect is given by the equation PPD=PD for each of the plots.

As seen from these figures, when air velocity is below about 0.08 m/s, the thermal sensation index PPD is in general more critical than the draught risk

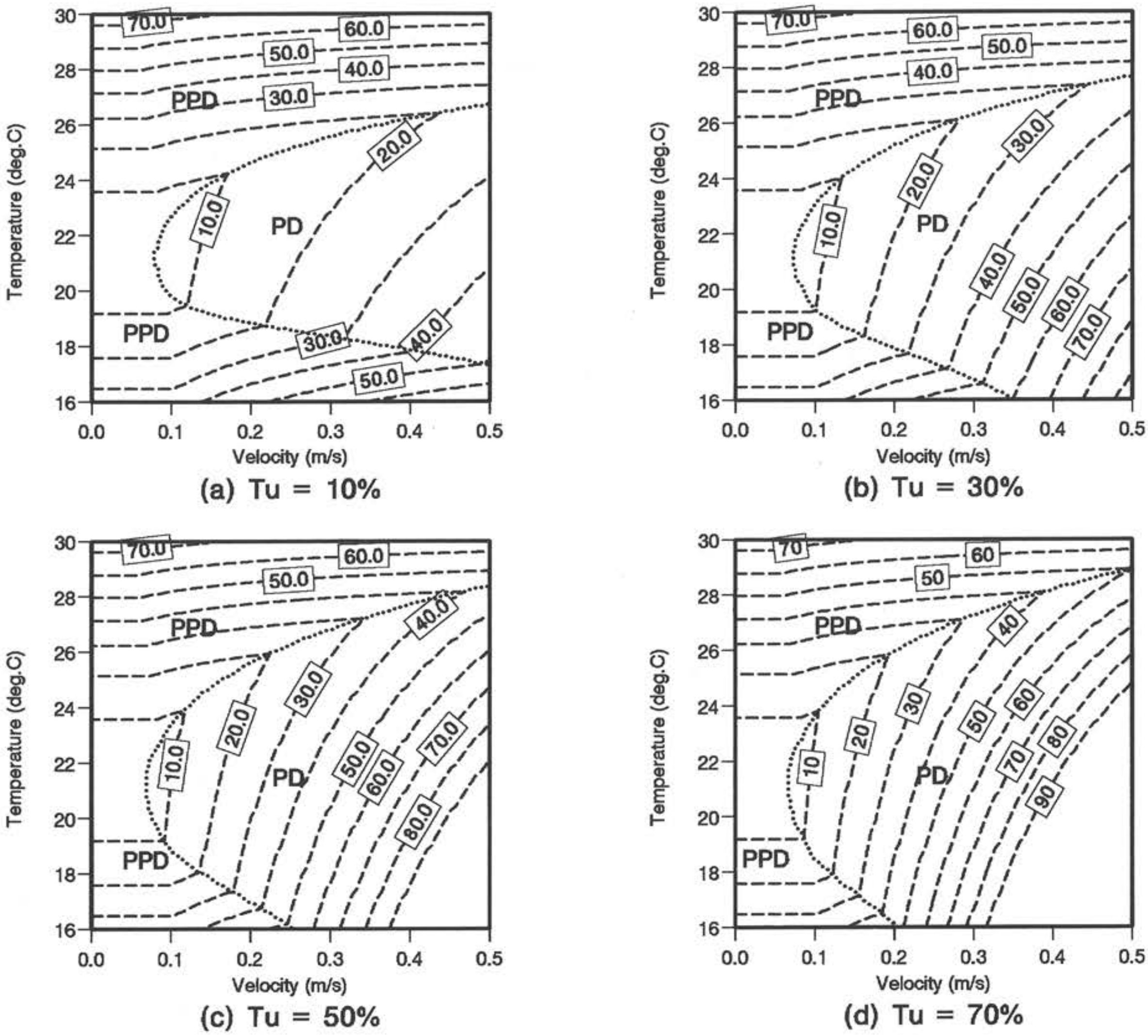

Fig. 8 Effect of air temperature and velocity on thermal comfort index Ψ=max [PPD, PD] for I_{cl}= 1.0 clo

and hence the draught risk in theory becomes more important, i.e. Ψ=PD, especially for air temperatures lower than the neutral temperature. For example, at an air velocity of 0.1 m/s and turbulence intensity of 50%, the range of air temperature for Ψ=PD increases from approximately 2.7 °C (22.5 to 25.2 °C) for I_{cl}=0.6 clo to 4.5 °C (19.0 to 23.5 °C) for I_{cl}=1.0 clo. Within these temperature ranges and at air velocities higher than 0.1 m/s, Ψ=PD and therefore it is not necessary to evaluate the thermal sensation level.

In naturally ventilated offices heated with radiators or convectors, air velocity is usually low (<0.08 m/s) and Ψ=PPD. Hence, the evaluation of thermal sensation is more important than the potential draught. In mechanically ventilated or air-conditioned offices, the air velocity in part of the space may be high so that Ψ=PD but due to non-uniform airflow, there may be some areas where either air velocity is low or air temperature deviates from neutrality so that Ψ=PPD. Therefore, the draught risk together with thermal sensation should be considered for a full assessment of thermal comfort.

Conclusions

A CFD program for direct assessment of thermal comfort (thermal sensation and draught risk as well as thermal discomfort due to asymmetric radiation or vertical temperature gradient) in rooms is described. The effect of the relevant environmental parameters on the thermal comfort is analysed. This study has shown that for accurate predictions of thermal comfort in occupied rooms the variations of not only the airflow pattern and air temperature but also the mean radiant temperature, water vapour pressure and turbulence intensity with space should be taken into account. For evaluation of thermal sensation alone, errors arising from taking the mean radiant temperature as a constant can be significant, particularly for rooms with a cold or hot surface such as a single glazed window or a radiant heating panel in winter. This is also true for thermal discomfort due to radiation asymmetry. Errors may also arise in predicting thermal sensation indices in occupied rooms when the variation of vapour pressure with space is disregarded.

A new index has been introduced to assess thermal comfort, Ψ=max [PPD, PD]. It can be used to judge whether PPD or PD needs to be included for a full assessment of thermal comfort in buildings. It has been found that in rooms with low air velocity ($V<0.08$ m/s and Ψ=PPD), evaluation of thermal sensation alone is normally sufficient to ensure thermal comfort, and the draught does not need to be assessed if the thermal sensation level is acceptable. In rooms where air velocity in part of the occupied zone is higher than 0.08 m/s (Ψ=PD), draught should be assessed together with thermal sensation levels for the space.

References

Anon. (1992a) *Proceedings of International Symposium on Room Air Conditioning and Ventilation Effectiveness,* Tokyo, Japan, July 22–24, 1992, Society of Heating, Air Conditioning and Sanitary Engineers of Japan.

Anon. (1992b) *Proceedings of Roomvent. '92 – Air Distribution in Rooms,* Aalborg, Denmark, September 2–4, 1992, Lyngby, Denmark, DANVAK.

ASHRAE (1981) *Thermal Environmental Conditions for Human Occupancy,* Atlanta, GA, American Society of Heating, Refrigerating and Air-Conditioning Engineers (ASHRAE Standard 55-1981).

ASHRAE (1985) *Handbook of Fundamentals,* Atlanta, GA, American Society of Heating, Refrigerating and Air-Conditioning Engineers.

Awbi, H. B. and Gan, G. (1991) "Computational fluid dynamics in ventilation". In: *Proceedings of CFD Seminar for Environmental and Building Services Engineers,* London, 26 November, 1991, Institute of Mechanical Engineers, pp. 67–79.

Chen, Q. (1990) "Comfort and energy consumption analysis in buildings with radiant panels", *Energy and Buildings,* **14**, (4), 287–297.

CIBSE (1986) "Environmental criteria for design". In: *CIBSE Guide A1,* London, Chartered Institute of Building Services Engineers.

Crisp, V. H. C., Fisk, D. J. and Sälvidge, A. C. (1984) "The BRE low energy office". In: *ECDPS Report,* Watford (UK), Building Research Establishment.

Fanger, P. O. (1982) *Thermal Comfort – Analysis and Applications in Environmental Engineering,* Florida, Robert E. Krieger Publishing Company.

Fanger, P. O., Melikov, A. K., Hanzawa, H. and Ring, J. (1988) "Air turbulence and sensation of draught", *Energy and Buildings,* **12**, 21–39.

Fanger, P. O. (1993) "How to apply models to thermal sensation and discomfort in practice". In: *Proceedings of Thermal Comfort: Past, Present and Future,* Watford, UK, 9–10 June, 1993, Building Research Establishment.

Gan, G., Awbi, H. B. and Croome, D. J. (1991) "Airflow and thermal comfort in naturally ventilated classrooms". In: *Proceedings of the 12th AIVC Conference,* Ottawa, Canada, September 24–27, 1991, Vol. 3, pp. 161–177.

Gan, G., Croome, D. J. and Awbi, H. B. (1993a) "Numerical prediction of contaminant distribution in ventilated rooms". In: Hughes, R. T., Goodfellow, H. D. and Rajhans, G. S. (eds) *Proceedings of Ventilation '91 – 3rd International Symposium on Ventilation for Contaminant Control,* Cincinnati, Ohio, USA, 12–20 September, 1991, pp. 359–366.

Gan, G., Awbi, H. B. and Croome, D. J. (1993b) "CFD simulation of the indoor environment for ventilation design". *Presented at the ASME 1993 Winter Meeting – Paper No. 93-WA/HT-49,* New Orleans, USA, November 28 – December 3, 1993.

ISO (1984) "Moderate thermal environments – determination of PMV and PPD indices and specifications of the conditions for thermal comfort". Geneva, International Standards Organisation, *(ISO 7730)*.

Jayatillaka, C. L. V. (1969) "The influence of Prandtl number and surface roughness on the resistance of the laminar sublayer to momentum and heat transfer", *Progress in Heat and Mass Transfer,* **1**, 193–329.

Launder, B. E. and Spalding, D. B. (1974) "The numerical computation of turbulent flows", *Computer Methods in Applied Mechanics and Engineering,* **3**, 269–289.

Leighton, D. J. and Pinney, A. A. (1990) "A set of standard office descriptions for use in modelling studies". In: *BEPAC Technical Note 90/5,* UK, Building Environmental Performance Analysis Club.

Leonard, B. P., (1979) "A stable and accurate convective modelling procedure based on quadratic upstream interpolation", *Computer Methods in Applied Mechanics and Engineering,* **19**, 59–98.

Patankar, S. V. (1980) *Numerical Heat Transfer and Fluid Flow,* Washington, Hemisphere Publishing Co.